Available online at www.sciencedirect.com
SCIENCE DIRECT®
ELSEVIER
Journal of Magnetism and Magnetic Materials 262 (2003) 111–115
Journal of magnetism and magnetic materials
www.elsevier.com/locate/jmmm

Blocking temperature distribution in implanted Co–Ni nanoparticles obtained by magneto-optical measurements

F. D'Orazio[a], F. Lucari[a,*], M. Melchiorri[a], C. de Julián Fernández[b], G. Mattei[b], P. Mazzoldi[b], C. Sangregorio[c], D. Gatteschi[c], D. Fiorani[d]

[a] *INFM—Dipartimento di Fisica, Università di L'Aquila, Via Vetoio 10-Coppito, I-67010 L'Aquila, Italy*
[b] *INFM—Dipartimento di Fisica, Università di Padova, Via Marzolo 8, 35131 Padova, Italy*
[c] *LAMM—Dipartimento di Chimica Polo Scientifico, Via della Lastruccia 3, 50019 Sesto Fiorentino (Fi), Italy*
[d] *ICMAT—CNR, Area della Ricerca di Roma, C.P. 10, 00016 Monterotondo, Rome, Italy*

Abstract

Three samples of Co–Ni alloy nanoparticles with different compositions were prepared by sequential ion implantation in silica slides. Transmission electron microscopy (TEM) showed the presence of spherical nanoparticles dispersed in the matrix. Magneto-optical Kerr effect analysis identified two magnetic components attributed to superparamagnetic particles in unblocked and blocked states, respectively. Magnetic field loops were measured as a function of temperature. Blocking temperature distributions were obtained; and their comparison with the size distributions derived from TEM provided the average magnetic anisotropy of the particles.

PACS: 75.50.Tt; 75.30.Gw; 78.20.Ls

Keywords: Co–Ni; Superparamagnetism; MOKE

1. Introduction

The production and characterization of nanostructurated materials with new properties is the most diffuse activity in the material science. A common method of modulating their magnetic features is throughout the realization of nanometric magnetic particle systems dispersed in a non-magnetic matrix. Frequently, particles made of pure elements are produced, whereas it is more difficult to obtain magnetic alloy grains. The sequential implantation of two different ionic species in a dielectric matrix is a process that, as a consequence of the atomic dynamics, allows the formation of small alloy particles dispersed in the matrix [1]. Their composition is controlled by the relative percentage of the implanted ions. In this work, we study the magnetic behaviour of Co–Ni particle samples produced by ion implantation in silica. We prepared samples with different compositions, with particular attention to Co-rich alloys, since their magnetic properties can be more enhanced. We studied their characteristics by transmission electron microscopy (TEM) and by

*Corresponding author. Tel.: +39-862-433098; fax: +39-862-433033.
E-mail address: franco.lucari@aquila.infn.it (F. Lucari).

0304-8853/03/$ - see front matter
doi:10.1016/S0304-8853(03)00030-1

magneto-optical Kerr effect (MOKE). The latter measures the rotation of the polarization plane of the light reflected by the surface of a magnetized specimen. The angle of rotation is proportional to the magnetization of the reflecting part of the sample.

2. Experiments and results

Silica slides (Heraeus Herasil) were sequentially implanted with Co^+ and Ni^+ ions at energy equal to 180 keV with a total flux of 15×10^{16} ions/cm^2. The Co^+ and Ni^+ doses were adjusted to obtain samples with 4:1, 2:1 and 1:1 Co:Ni ratio (Table 1). TEM analysis was performed with a Philips CM30T, operating at 300 kV, on cross sectional samples thinned with an Ar^+-ion milling system at liquid nitrogen temperature. These studies showed that the implantation produces spherical nanoparticles with composition and crystalline structure similar to the corresponding bulk alloys [2,3]. The average diameters D of the particles are reported in Table 1.

The magnetic characterization was performed by MOKE in longitudinal configuration, as a function of the magnetic field, in the temperature interval 10–300 K. The wavelength of the light was 0.63 nm. The measurements show well-defined hysteresis loops. The low-temperature results are reported in Fig. 1.

The MOKE loops often are characterized by a peculiar shape with a narrowing of the cycle at low magnetic field. This feature can be interpreted by decomposing all the MOKE results according to the model illustrated in Ref. [4] which considers the magnetic contribution of the blocked and superparamagnetic nanoparticles. The hysteresis loops are analysed utilizing the phenomenological expression:

$$\theta = B_{sp}L(C_{sp}H) + B_{bl}L[C_{bl}(H \pm H_C)], \quad (1)$$

where $L(x) = \coth(x) - 1/x$ is the Langevin function. The first term describes a superparamagnetic contribution and the second one approximates the magnetic behaviour of blocked particles. In Fig. 2, an example of this decomposition is reported.

The values of H_C vs. temperature are reported in Fig. 3 for all the samples. In the inset, as an example, we show the comparison for sample 4:1 between the value of H_C obtained from the fit and the value aquired directly from the measurements and defined as the magnetic field corresponding to zero MOKE response. The difference depends on

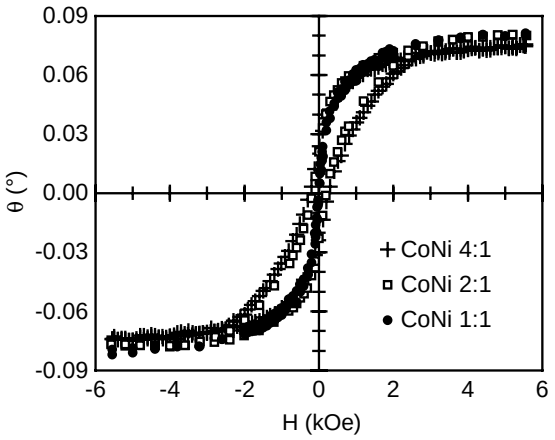

Fig. 1. MOKE hysteresis loops measured at 10 K. The linear contribution of the cryostat windows and the silica matrix have been subtracted. We remark that the saturation does not change from sample to sample, whereas, as the temperature is raised up to 300 K, only about a 10% decrease is observed.

Table 1
Structural and magnetic parameters of the samples

Sample	D (nm)	H_C (0) (Oe)	T_f (K)	α	T_0 (K)	σ_T (K)	K (10^5 J/m^3)
CoNi	3.8	120	32	2.65	23.4	1.35	1.4
Co_2Ni	2.9	800	137	0.34	49.9	1.88	3.6
Co_4Ni	2.5	724	81	0.59	46.0	1.53	7.6

D is the average particle diameter from TEM; $H_C(0)$, T_f and α are the parameters of Eq. (2); T_0 and σ_T the parameters of the BTD; and K the estimated average magnetic anisotropy constant.

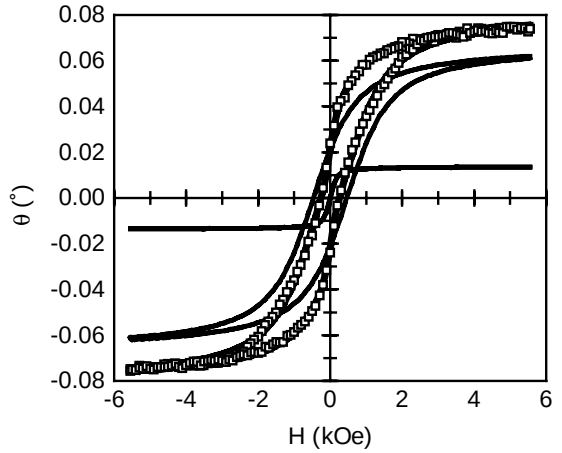

Fig. 2. Decomposition of the experimental MOKE loop for sample 4:1 measured at 10 K. The data points (□) are fitted according to Eq. (1) with the solid line superimposed to the data. The other two solid curves are the components of the blocked (the one with hysteresis) and unblocked particles (the lower one).

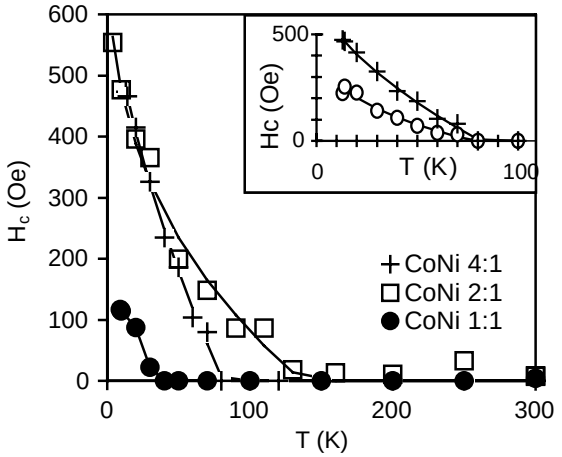

Fig. 3. Temperature dependence of the coercivity for the blocked component of the samples. In the inset the comparison, for sample 4:1, between the coercivity of the blocked component (+) and the coercivity of the overall hysteresis MOKE loops (○) is presented.

the relevant contribution of the unblocked particles.

The temperature dependence of H_C is well described by

$$H_c(T) = H_c(0)\,[1 - (T/T_f)^{\alpha}]$$

(full line in Fig. 3) [5] with the parameters reported in Table 1.

It can be useful to note that the values of α are affected by a large experimental error, as deduced from the dispersion of the experimental points in Fig. 3. However, the difference between our estimates and the value of α predicted by the Stoner–Wolfarth theory depends principally on the fact that our particles are not necessarily uniaxial and, most of all, they are not identical.

3. Blocking temperature and size distributions

At all temperatures, from the fitted hysteresis cycles, we estimated the remanence-to-saturation ratio $S = M_{rem}/M_{sat}$. With a best fit from these data, we obtained the blocking temperature distribution (BTD) [6]

$$f(T) = -\frac{dS}{dT}$$

assuming that it is well approximated by a log-normal function:

$$f(T) = \frac{A}{T\sqrt{2\pi(\ln\sigma_T)^2}}\exp\left[-\frac{1}{2}\left(\frac{\ln T - \ln T_0}{\ln\sigma_T}\right)^2\right],$$

where $\ln T_0$ and $\ln\sigma_T$ are the mean value and the standard deviation of the variable $\ln T$, respectively. For each sample we report the values in Table 1. The values of T_0 refer to the blocking temperature of the average size particles and they are correctly lower than the corresponding values of T_f which are related to the blocking temperature of the biggest particles. Moreover, it is interesting to observe that the BTD of samples Co_4Ni and Co_2Ni have a very similar mean value, although the width is greater for sample Co_2Ni. On the contrary, the distribution for sample CoNi shows a smaller mean value and a lower width. This fact testifies that the particles with the 1:1 composition have smaller anisotropy energy than those present in the other samples, since the energy necessary to unblock the first particles is smaller.

From $f(T)$ we determined the volume distribution functions, $F_{MOKE}(V)$: we performed a change of variable using the Néel relaxation time model

[5] which asserts a connection between the volume V of a particle and its blocking temperature:

$$T_B = \frac{KV}{k_B \ln(\tau_m/\tau_0)},$$

where K is the average magnetic anisotropy constant, τ_m the measurement time of the MOKE experiment (5 s), and τ_0 is a constant of the order of 10^{-9} s for ferromagnetic materials. We therefore get

$$F_{MOKE}(V) = \frac{K}{22k_B} f\left(\frac{KV}{22k_B}\right).$$

Finally, we imposed a correspondence between the $F_{MOKE}(V)$ of all samples with the volume distribution acquired by TEM measurements [3]. This is done by deriving a volume-weighted distribution function $F_{TEM}(V)$ from the TEM particle size distribution. $F_{TEM}(V)$ is compared with $F_{MOKE}(V)$ defined above, after choosing the proper value of the scale factor which multiplies V in the argument of the function f. This value is the one which minimizes the deviation between the two distribution functions (plotted in Fig. 4) and, therefore, provides a best value of K. The estimated average magnetic anisotropy constants for the three samples are reported in the last column of Table 1. These are larger than the corresponding values in bulk but comparable in the order of magnitude [7]. However, the presence in this case of contributions like shape, surface or stress anisotropy can account for the differences.

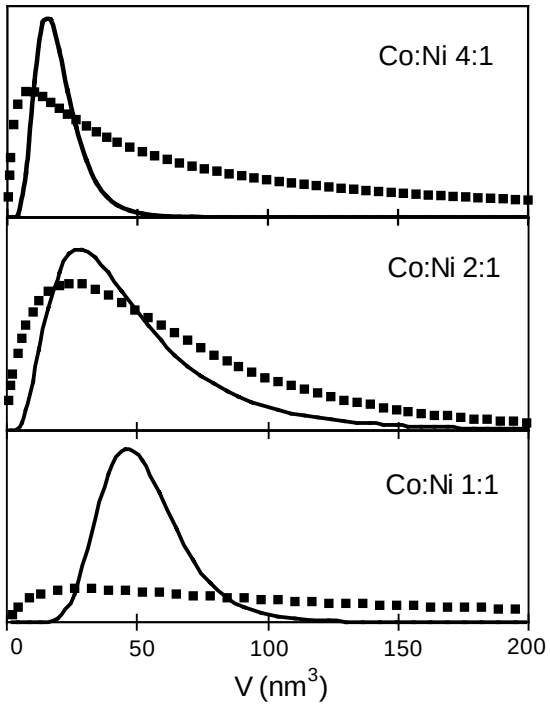

Fig. 4. Comparison between the particle volume distributions obtained from MOKE (——) and TEM (■).

The smaller values of K for CoNi confirm that, although formed by bigger particles, the sample unblocks at lower temperature. Such a result can be connected with structural observations that indicate cubic symmetry for sample CoNi, but hexagonal order in the alloys Co_4Ni and Co_2Ni. From Fig. 4, the agreement between the two distributions is better for samples 4:1 and 2:1. Moreover, the MOKE distribution is usually narrower than the distribution from TEM. This may be due to interparticle magnetic interactions that cause a more cooperative response of the blocking–unblocking process. If this were the case, in the MOKE distribution it would be necessary to use a larger effective volume than the one obtained by TEM. For this reason, our values of K may be overestimated.

4. Conclusions

Co–Ni alloy particles with different compositions were prepared by sequential ion implantation. The magnetic properties were investigated, identifying two contributions to the hysteresis loop due to superparamagnetic particles in blocked and unblocked states, respectively. The composition-dependent coercive field and saturation were related to the different properties of the corresponding bulk alloys. Finally, the BTD was compared with the TEM particle size distribution and the anisotropy constant was obtained.

References

[1] F. Gonella, P. Mazzoldi, in: H. Singh Nalwa (Ed.), Handbook of Nanostructured Materials and Nanotechnology, Vol. 1, Academic Press, San Diego, 2000, p. 81.

[2] C. de Julián Fernández, C. Sangregorio, G. Mattei, G. De, A. Saber, S. Lo Russo, G. Battaglin, M. Catalano, E. Cattaruzza, F. Gonella, D. Gatteschi, P. Mazzoldi, Mater. Sci. Eng. C15 (2001) 59.
[3] C. Maurizio, A. Longo, A. Martorana, E. Cattaruzza, F. D'Acapito, F. Gonella, C. de Julián, G. Mattei, P. Mazzoldi, S. Padovani, P. Boesecke, unpublished.
[4] F. D'Orazio, F. Lucari, C. de Julián, G. Mattei, S. Lo Russo, C. Maurizio, P. Mazzoldi, C. Sangregorio, D. Gatteschi, F. Gonella, E. Cattaruzza, C. Battaglin, D. Fiorani, J. Magn. Magn. Mater. 242–245 (2002) 627.
[5] J.L. Dormann, D. Fiorani, E. Tronc, Adv. Chem. Phys. 98 (1997) 283.
[6] R.W. Chantrell, K. O'Grady, in: R. Gerber, et al., (Eds.), Applied Magnetism, Kluwer Academic Publishers, Amsterdam, 1994, p. 113.
[7] H.P.J. Wijn (Ed.), Magnetic Properties of Metals, Springer, New York, 1991, p. 38.